Inorganic Chemistry

Article

pubs.acs.org/IC

Electrochemiluminescent Peptide Nucleic Acid-Like Monomers Containing Ru(II)−Dipyridoquinoxaline and Ru(II)−Dipyridophenazine Complexes

Tanmaya Joshi,[†] Gregory J. Barbante,[‡] Paul S. Francis,[‡] Conor F. Hogan,[§] Alan M. Bond,[†] and Leone Spiccia*[,†]

[†]ARC Centre of Excellence for Electromaterials Science and School of Chemistry, Monash University, Clayton, Victoria 3800, Australia

[‡]School of Life and Environmental Sciences, Deakin University, Geelong, Victoria, 3217, Australia

[§]Department of Chemistry, La Trobe Institute for Molecular Science, La Trobe University, Victoria, 3086, Australia

Supporting Information

ABSTRACT: A series of Ru(II)−peptide nucleic acid (PNA)-like monomers, $[Ru(bpy)_2(dpq\text{-}L\text{-}PNA{-}OH)]^{2+}$ (**M1**), $[Ru(phen)_2(dpq\text{-}L\text{-}PNA{-}OH)]^{2+}$ (**M2**), $[Ru(bpy)_2(dppz\text{-}L\text{-}PNA{-}OH)]^{2+}$ (**M3**), and $[Ru(phen)_2(dppz\text{-}L\text{-}PNA{-}OH)]^{2+}$ (**M4**) (bpy = 2,2′-bipyridine, phen = 1,10-phenanthroline, dpq-L-PNA−OH = 2-(N-(2-(((9H-fluoren-9-yl)methoxy)-carbonylamino)ethyl)-6-(dipyrido[3,2-*a*:2′,3′-*c*]phenazine-11-carboxamido)hexanamido)acetic acid, dppz-L-PNA−OH = 2-(N-(2-(((9H-fluoren-9-yl) methoxy)carbonylamino)ethyl)-6-(dipyrido[3,2-*f*:2′,3′-*h*]quinoxaline-2-carboxamido)acetic acid) have been synthesized and characterized by IR and ^{1}H NMR spectroscopy, mass spectrometry, and elemental analysis. As is typical for Ru(II)−tris(diimine) complexes, acetonitrile solutions of these complexes (**M1**−**M4**) show MLCT transitions in the 443−455 nm region and emission maxima at 618, 613, 658, and 660 nm, respectively, upon photoexcitation at 450 nm. Changes in the ligand environment around the Ru(II) center are reflected in the luminescence and electrochemical response obtained from these monomers. The emission intensity and quantum yield for **M1** and **M2** were found to be higher than for **M3** and **M4**. Electrochemical studies in acetonitrile show the Ru(II)−PNA monomers to undergo a one-electron redox process associated with Ru^{II} to Ru^{III} oxidation. A positive shift was observed in the reversible redox potentials for **M1**−**M4** (962, 951, 936, and 938 mV, respectively, vs $Fc^{0/+}$ (Fc = ferrocene)) in comparison with $[Ru(bpy)_3]^{2+}$ (888 mV vs $Fc^{0/+}$). The ability of the Ru(II)−PNA monomers to generate electrochemiluminescence (ECL) was assessed in acetonitrile solutions containing tripropylamine (TPA) as a coreactant. Intense ECL signals were observed with emission maxima for **M1**−**M4** at 622, 616, 673, and 675 nm, respectively. At an applied potential sufficiently positive to oxidize the ruthenium center, the integrated intensity for ECL from the PNA monomers was found to vary in the order **M1** (62%) > **M3** (60%) > **M4** (46%) > **M2** (44%) with respect to $[Ru(bpy)_3]^{2+}$ (100%). These findings indicate that such Ru(II)−PNA bioconjugates could be investigated as multimodal labels for biosensing applications.

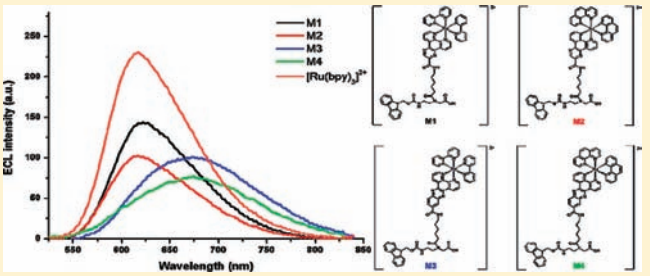

INTRODUCTION

Peptide nucleic acids (PNA)—artificial DNA analogues assembled on the N-(2-aminoethyl)-glycine backbone—have fascinated researchers throughout the past two decades due to their potential therapeutic applications.[1−9] They possess inherent specificity and strong affinity for Watson−Crick base pairing for cDNA or RNA strands, partly attributed to the lack of electrostatic repulsion.[2,10,11] The neutral polyamide backbone not only contributes to the hybridization stability but also makes PNA resistant to both proteases and nucleases.[4,12] These properties are particularly attractive for antisense and antigene therapies, as well as for diagnostic and analytical applications in biosensing areas.[7−9,13−15] To further diversify the applications of PNA, the native molecule has been subjected to numerous modifications aimed at improving the innate physical and chemical properties as well as introducing new functionalities and spectroscopic characteristics. Thus, the field of PNA−metal bioconjugates has been advancing rapidly since the concept was first introduced.[16−19] Incorporation of metal complexes into the PNA oligomer allows tailoring of properties to achieve particular desired objectives. PNA−metal bioconjugates present themselves as very promising candidates for electrochemical, radiochemical, and optical biosensing and can also be employed to confer and/or influence hybridization stability in the formed duplexes.[16,18−24] Examples of metal−PNA oligomers/monomers incorporating ferrocene, Re(II), Ru(II), Zn(II), Cu(II), Zr(IV), Mn(III), Co(II) and ^{99m}Tc derivatives have been

Received: September 1, 2011
Published: October 31, 2011

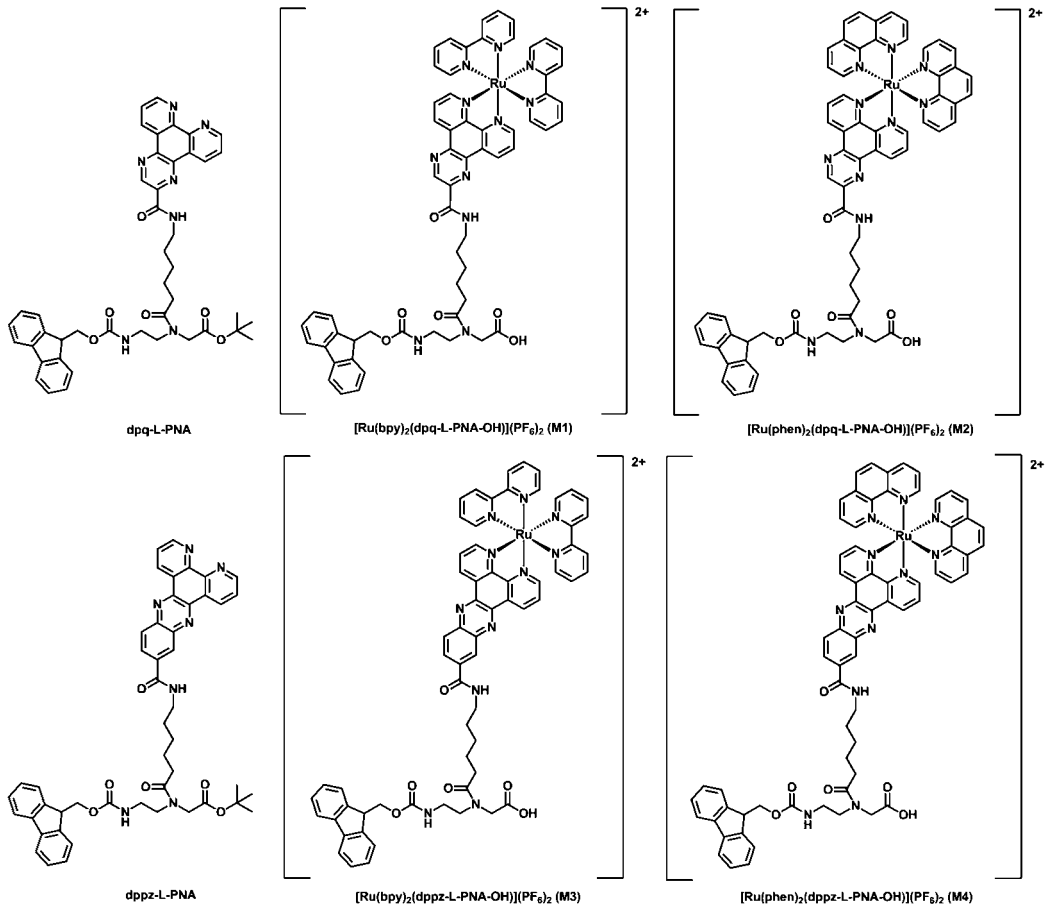

Figure 1. Structures of the dpq-L-PNA and dppz-L-PNA ligands and **M1**−**M4**.

reported in the literature.[19,24−34] As first described by Metzler-Nolte et al.,[17,18] covalent attachment of metal complexes to the reactive N-terminus of the PNA sequence represents the classical approach for metal insertion, but it limits the degree of flexibility achievable in metal−PNA oligomers. This restriction has led to the development of new classes of metal-containing PNA monomers for direct insertion into the desired location within the PNA oligomers.[19,28,35−37] However, while there are many examples of such monomers in the literature, as far as we are aware, the only successful insertion of a metal complex within the desired PNA oligomer on a solid phase is contained in reports by Metzler-Nolte and co-workers.[32,38,39] In these studies, ferrocenyl−PNA bioconjugates were prepared by employing "click chemistry" between the alkyne-containing PNA oligomer and the corresponding azido-ferocene derivative.[32,38,39] Similarly, ^{99m}Tc tricarbonyl-containing PNA oligomers were prepared using a related "click chemistry" approach to create a metal complexation site on the oligomeric unit which was converted into a ^{99m}Tc tricarbonyl derivative.[34] To date, this approach for insertion of the metal complex is the main route explored for the synthesis of ferrocenyl−PNA oligomers. Significantly, the stability of the ferrocenyl group and its large derivatives library make it an excellent choice for electrochemical biosensors.[40,41] Nevertheless, it is also desirable to prepare PNA−metal bioconjugates that widen the scope of biosensor applications by allowing multiple detection probes. Polypyridyl−Ru(II) complexes, for example, provide attractive electrochemical and photochemical properties and hence represent suitable contenders for dual detection probes. Due to their high chemical, thermal, and photochemical stability; reversible redox behavior; intense UV−visible absorption with long-lived MLCT excited states; and large Stoke shifts, Ru(II) polypyridyl complexes play an important role in a variety of biosensing applications based on photoluminescence, chemiluminescence (CL), and electrochemiluminescence (ECL).[42−59]

In order to advance the dual sensing field, we have been interested in introducing a robust framework of Ru(II)−PNA monomers, which can be inserted into any selected position within the PNA sequences.[37] Our initial work showed that (as expected) the required characteristic electrochemical and photochemical properties of the Ru(II)−PNA monomers remain more or less unperturbed when conjugated onto the PNA backbone, but major synthetic and purification difficulties were encountered. Previous synthetic shortcomings are now addressed by designing new types of Ru(II)−polypyridyl-based PNA-like monomers that allow easy insertion into the oligomeric sequences. Photoluminescence and electrochemical and ECL responses are then explored. In particular, the synthesis of two novel PNA derivatives, dpq-L-PNA, dppz-L-PNA, and their Ru(II)−bis(bipyridyl)/bis(phenanthroline) complexes, **M1**, **M2**, **M3**, and **M4** (Figure 1), is described. Monomers **M1** and **M2** are assembled around the dipyridoquinoxaline (dpq) backbone using dpq-L-PNA, whereas dppz-L-PNA, which bears the dipyridophenazine (dppz) unit, is used in the cases of **M3** and **M4**. The ligands are attached to the PNA monomer backbone via a hexyl linker to provide steric flexibility. While photophysical and electrochemical properties

dx.doi.org/10.1021/ic201911f | *Inorg. Chem.* 2011, 50, 12172−12183

of Ru(II)−PNA monomers/oligomers have previously been reported,[17,37] to the best of our knowledge, this is the first study of the electrochemiluminescent properties of PNA-like monomers with conjugated ECL active compounds.

EXPERIMENTAL SECTION

Chemicals. Unless otherwise stated, the chemicals were either of reagent or analytical grade quality and were used as purchased from the manufacturer. 2,3-Bis(*tert*-butoxycarbonylamino)propanoic acid (**1**),[60] ethyl-6-aminohexanoate hydrochloride,[61] 1,10-phenanthroline-5,6-dione (**9**),[62] *tert*-butyl-2-(2-(((9H-fluoren-9-yl)methoxy)-carbonylamino)ethylamino) acetate hydrochloride (**8**),[63] Ru(bpy)$_2$Cl$_2$,[64] and Ru(phen)$_2$Cl$_2$[64] were synthesized according to literature procedures. Characterization data were in agreement with literature reports. When required, solvents for the synthetic work were degassed by purging with dry, oxygen-free nitrogen for at least 30 min before use. Acetonitrile was dried before use by standing over calcium hydride overnight. Deionized water was used for all reactions undertaken in aqueous media. HPLC-grade solvents were used for all spectral studies. Tetrabutylammonium hexafluorophosphate (nBu$_4$NPF$_6$, Fluka) was recrystallized prior to use as the electrolyte for the electrochemical studies in MeCN.[65]

Instrumentation and Methods. A vacuum line and Schlenk glassware were employed when reactions had to be carried out under an atmosphere of dry, oxygen-free nitrogen. Protection from light was provided if necessary by wrapping the assemblies with aluminum foil. ^{1}H and ^{13}C NMR spectra were obtained with Bruker AC200, AM300, or DRX 400 spectrometers and referenced against tetramethylsilane (TMS) or signals from the residual protons of deuterated solvents.[66] The chemical shifts, δ, are reported in parts per million (ppm) relative to the reference, and coupling constants, J, are given in Hertz. Peak multiplicities are abbreviated as follows: s (singlet), d (doublet), t (triplet), and m (multiplet). ESI mass spectra were recorded using a Micromass Platform II mass spectrometer fitted with an ESI source (capillary voltage 3.5 eV and cone voltage 35 V). The most intense m/z value is listed. Accurate high-resolution mass spectra were obtained with a Bruker BioApex II 47e FT-ICR MS instrument fitted with an Analytica Electrospray Source. Samples were introduced by a syringe pump at a rate of 1 μL min^{-1}, and the capillary voltage was 200 V. Infrared spectra were recorded from KBr disks or neat as indicated, using a Perkin-Elmer 1600 Series FTIR spectrometer in the range 4000−500 cm^{-1} with a resolution of ±4.0 cm^{-1}. Peak intensities are given as broad (br), very strong (vs), strong (s), medium (m), and weak (w). Microanalyses were carried out by the Campbell Microanalytical Laboratory, University of Otago, New Zealand. UV/vis spectra were recorded using Varian Cary Bio 300 or 5G spectrophotometers. Photoluminescence spectra were obtained with a Fluoromax-4 spectrofluorometer (Horiba Jobin Yvon Inc.), following excitation at 450 nm, and were autocorrected for instrumental response using a correction factor provided by the instrument manufacturer. The excitation and emission slit width for recording the emission spectra were set to 3.0 and 2.5 nm, respectively. UV/visible and emission spectra were measured using a 10 μM acetonitrile solution of each complex at 25 °C in 1 cm quartz cuvettes. All solutions were degassed by purging with nitrogen. Thin layer chromatography (TLC) was performed using silica gel 60 F-254 (Merck) plates with detection of spots achieved either by exposure to iodine or UV light or by using ninhydrin stain. Column chromatography was undertaken using silica gel 60 (0.040−0.063 mm mesh, Merck). Eluent mixtures are expressed as volume to volume (v/v) ratios.

Electrochemical Measurements. Cyclic voltammetric measurements were performed at (20 ± 2)°C in acetonitrile solutions containing 0.1 M nBu$_4$NPF$_6$ as the supporting electrolyte, over the scan rate range of 100−1000 mV s^{-1} using a BAS 100B (Bioanalytical Systems) electrochemical workstation. Solutions used in electrochemical measurements were deoxygenated by purging with high purity nitrogen for at least 10 min before commencing the experiments. A conventional three electrode cell was employed which comprised a glassy carbon working electrode (area = 0.0079 cm^2), a large surface area Pt counter electrode, and a Ag/Ag$^+$ (0.1 M $AgNO_3$ in CH_3CN) reference electrode. The potential of the Ag/Ag$^+$ reference electrode was frequently calibrated against that of the ferrocene/ferrocinium ($Fc^{0/+}$) redox couple by measuring the reversible potential derived from oxidation of Fc under identical conditions used for the voltammetric measurements on the Ru(II) complexes. The working electrode was polished with an aqueous slurry of aluminum oxide (0.3 μm), then rinsed with acetone and dried before each voltammetric experiment.

Electrochemiluminescence experiments were undertaken with a PGSTAT 12 Autolab electrochemical workstation (MEP Instruments, North Ryde, NSW, Australia) in combination with General Purpose Electrochemical Systems (GPES) software (version 4.9). In these studies, the electrochemical cell consisted of a glass cell with a quartz base. The cell was enclosed in a custom-built light-tight faraday cage. A three-electrode configuration, consisting of a 3 mm-diameter glassy carbon working electrode shrouded in Teflon (CH Instruments, Austin, TX, USA), a 1 cm^2 platinum gauze auxiliary electrode, and a silver wire quasi reference electrode, was used. ECL spectra were obtained using an Ocean Optics CCD spectrometer, model QE65000, coupled to the cell with a 1 m fiber optic cable. The spectral acquisition was triggered simultaneously with the electrochemical experiment with the aid of an HR 4000 breakout box (Ocean Optics). The Ru(II) complexes were prepared at a concentration of 0.1 mM in freshly distilled acetonitrile, with 0.1 M nBu$_4$NPF$_6$ as the supporting electrolyte and 0.1 M tripropylamine as the ECL coreactant. Prior to each experiment, the working electrode was polished sequentially with slurries of 0.3 and 0.05 μm alumina on a felt pad, sonicated in water (1 min), rinsed in freshly distilled acetonitrile, and dried with a stream of nitrogen. The working electrode was then positioned *ca.* 2 mm from the bottom of the cell for detection of the ECL signal, and the solution was purged with argon for 3 min. ECL intensities are given relative to [Ru(bpy)$_3$](PF$_6$)$_2$ (100%) measured under the same conditions. To generate the emission, the working electrode was pulsed for 2.0 s between 0 V and a value sufficiently positive to generate the ruthenium(III) complex in each case. The resulting ECL spectra were collected over the duration of three such chronoamperometric cycles.

Synthesis. *Ethyl-6-(2,3-bis(tert-butoxycarbonylamino)-propanamido)hexanoate (**2**).* DCC (0.255 g, 1.24 mmol), HOBt (0.165 g, 1.20 mmol), and DMAP (20 mg) were added to a solution of 2,3-bis(*tert*-butoxycarbonylamino)propanoic acid (**1**; 0.250 g, 0.822 mmol) in THF (10 mL). The resulting suspension was stirred at room temperature under nitrogen for 2 hours. Ethyl-6-aminohexanoate solution (prepared by treating ethyl-6-aminohexanoate hydrochloride (0.250 g, 1.30 mmol) with triethylamine (0.130 g, 1.60 mmol) in 10 mL dry acetonitrile) was then added dropwise, and stirring was continued for 16 h under nitrogen. The reaction mixture was filtered through a small celite pad. The celite pad was washed thoroughly with dichloromethane and the filtrate concentrated under reduced pressure. The solid residue was dissolved in dichloromethane (60 mL) and filtered. The filtrate was washed with 10% citric acid (3 × 25 mL), saturated $NaHCO_3$ (3 × 25 mL), water (1 × 20 mL), and brine (1 × 20 mL). The organic phase was then dried over anhydrous Na_2SO_4 and filtered and the filtrate evaporated to dryness to obtain **2** as a white solid. Yield: 0.265 g (75%). R_f = 0.50 in 5% MeOH/DCM. IR (KBr): ν 3375s (N−H), 3293s (N−H), 2939s (C−H$_{aliph}$), 2866m (C−H$_{aliph}$), 1734s (C═O), 1718s (C═O), 1701s (C═O), 1527m, 1459w, 1390w, 1369m, 1305m, 1281m, 1253m, 1198m, 1165s, 1098m, 1025w, 870s cm^{-1}. ^{1}H NMR (300 MHz, $CDCl_3$): δ 4.21−4.08 (m, 3H), 3.44−3.23 (m, 4H), 2.26−2.23 (m, 2H), 1.89−1.58 (m, 4H), 1.42 (s, 9H), 1.39−1.22 (m, 14H) ppm. ^{13}C NMR (75 MHz, $CDCl_3$): δ 173.9, 170.8, 157.1, 80.7, 80.3, 60.6, 49.4, 39.5, 34.4, 29.4, 28.7, 28.6, 26.6, 25.9, 24.8, 14.5 ppm. MS (ESI$^+$): m/z 468.3 [M + Na]$^+$.

*Ethyl-6-(2,3-diaminopropanamido)hexanoate (**3**).* Ethyl-6-(2,3-bis(*tert*-butoxycarbonylamino)propanamido)hexanoate (**2**; 0.223 g, 0.50 mmol) was dissolved in DCM/trifluoroacetic acid (1:1, 5 mL) and the solution stirred at room temperature for 5 h. The solvent was evaporated under reduced pressure, and the residue was triturated with toluene and ether to obtain the trifluoroacetic acid salt of **3** as a brown

dx.doi.org/10.1021/ic201911f | *Inorg. Chem.* 2011, 50, 12172−12183

solid. Yield: 0.230 g (98%). IR (KBr): ν 3328s (N−H), 2929s (C−H_{aliph}), 2851s (C−H_{aliph}), 1693s (C═O), 1653s (C═O), 1578m, 1312m, 1272w, 1244m, 1205w, 1158w, 1088m, 892m cm^{-1}. ^1H NMR (300 MHz, CD_3OD): δ 4.22−4.18 (m, 1H), 4.09 (q, ^3J = 7.1 Hz, 2H), 3.44−3.35 (m, 3H), 3.25−3.14 (m, 1H), 2.30 (t, ^3J = 7.3 Hz, 2H), 1.71−1.51 (m, 4H), 1.36−1.31 (m, 2H), 1.22 (t, ^3J = 7.1 Hz, 3H) ppm. ^{13}C NMR (75 MHz, CD_3OD): δ 174.4, 165.9, 60.3, 48.6, 39.7, 33.6, 28.5, 26.2, 25.6, 24.4, 13.4 ppm. MS (ESI^+): m/z 246.1 $[M + H]^+$.

*6-(Pyrazino[2,3][1,10]phenanthroline-2-carboxamido)hexanoic Acid (**4**).* 1,10-Phenanthroline-5,6-dione (0.074 g, 0.350 mmol) was added to absolute ethanol (10 mL) and the mixture refluxed to complete the dissolution. A solution of ethyl-5-(2,3-diaminopropanamido)hexanoate (**3**; 0.212 g, 0.450 mmol) in absolute ethanol (10 mL) was then added, and the reaction mixture was refluxed. Monitoring by TLC indicated completion of the reaction after 5 h. The reaction mixture was cooled to room temperature. The small amount of yellow precipitate was filtered, and the filtrate was evaporated to dryness to obtain a reddish orange solid (115 mg) as the crude product. The crude product was dissolved in 8 mL of MeOH/H_2O (3:1) and solid NaOH (0.042 g, 1.10 mmol) added at 0 °C. After stirring overnight at room temperature for 16 h, the volume of the reaction mixture was reduced to 4 mL by rotary evaporation. The alkaline solution was acidified to pH 3 using 1 M HCl and evaporated to dryness. The resulting solid was purified by column chromatography (SiO_2, 10% MeOH/DCM) to obtain **4** as a white solid. Yield: 0.085 g (63%). R_f = 0.20 in 10% MeOH/DCM. IR (KBr): ν 3410w (N−H), 3058w (C−H_{arom}), 2929m (C−H_{aliph}), 2855m (C−H_{aliph}), 1720s (C═O), 1670s (C═O), 1533m, 1432w, 1402m, 1390m, 1376m, 1261w, 1246m, 1202s, 1159m, 1128w, 1076w, 940m, 823m, 742s cm^{-1}. ^1H NMR (300 MHz, DMSO-d_6): δ 9.56 (s, 1H), 9.40−9.38 (m, 2H), 9.23−9.22 (m, 2H), 7.96−7.90 (m, 2H), 3.45−3.38 (m, 2H), 2.24 (t, ^3J = 7.1 Hz, 2H), 1.63−1.51 (m, 4H), 1.47−1.39 (m, 2H) ppm. ^{13}C NMR (75 MHz, DMSO-d_6): δ 175.2, 163.4, 153.3, 153.0, 148.1, 147.8, 144.8, 144.0, 141.8, 138.6, 134.5, 133.6, 127.0, 126.8, 125.2, 124.9, 41.2, 34.4, 29.9, 26.9, 25.1 ppm. MS (ESI^-): m/z 388.1 $[M - H]^-$.

*tert-Butyl-2-(N-(2-(((9H-fluoren-9-yl)methoxy)carbonylamino)-ethyl)-6-(dipyrido[3,2-f:2′,3′-h]quinoxaline-2-carboxamido)-hexanamido)acetate (**dpq-L-PNA**).* 6-(Pyrazino[2,3][1,10]-phenanthroline-2-carboxamido)hexanoic acid (**4**; 0.120 g, 0.308 mmol) was suspended in dry DMF (5 mL) under nitrogen. HBTU (0.243 g, 0.616 mmol) and DMAP (20 mg) were added to the suspension, and the reaction mixture was stirred at room temperature for 30 min. *tert*-Butyl-2-(2-(((9H-fluoren-9-yl)methoxy)-carbonylamino)ethylamino)acetate hydrochloride (0.277 g, 0.640 mmol) was added, and stirring continued at room temperature for a further 15 min. Diisopropylethylamine (0.11 mL, 0.60 mmol) was added dropwise at 0 °C. After the reaction mixture was stirred for 30 min at 0 °C, it was stirred at room temperature for a further 18 h. Water (25 mL) was then added, resulting in the formation of a precipitate which was collected by filtration. The precipitate was dissolved in dichloromethane, the solution dried over Na_2SO_4, filtered, and concentrated to obtain the crude product, which was purified by column chromatography (SiO_2, gradual change of eluent polarity from 100% EtOAc to 10% MeOH/DCM) to afford **dpq-L-PNA** as a pale yellow solid. Yield: 0.165 g (73%). R_f = 0.45 in 10% MeOH/DCM. IR (KBr): ν 3067w (C−H_{arom}), 3014w (C−H_{arom}), 2930s (C−H_{aliph}), 2855m (C−H_{aliph}), 1730s (C═O), 1655s (C═O), 1535br, 1459m, 1399m, 1377w, 1252s, 1235m, 1199w, 1156s, 1079w, 1035w, 1017w, 848m, 760m, 743s cm^{-1}. ^1H NMR (300 MHz, $CDCl_3$): mixture of rotamers δ 9.74−9.71 (m, 1H), 9.49−9.26 (m, 4H), 8.08−7.86 (rotamers, m, 1H), 7.83−7.73 (m, 2H), 7.68−7.66 (m, 1H), 7.55−7.46 (m, 3H), 7.33 (t, ^3J = 7.4 Hz, 1H), 7.25−7.15 (rotamers, m, 3H), 4.33−4.30 (m, 2H), 4.12 (q, ^3J = 7.4 Hz, 1H), 3.97−3.93 (rotamers, m, 2H), 3.66−3.38 (m, 6H), 2.46−2.25 (m, 2H), 1.75−1.70 (m, 4H), 1.50−1.43 (m, 11H) ppm. ^{13}C NMR (75 MHz, $CDCl_3$): mixture of rotamers δ 174.5, 173.8, 170.0 (min) and 169.1 (maj), 163.3 (min) and 163.2 (maj), 156.9, 153.3 (min) and 153.2 (maj), 153.0, 152.9, 148.1, 148.0, 144.2 (maj) and 144.1 (min), 144.0, 143.9, 143.6, 142.5, 141.5, 141.2, 138.1, 134.0, 133.3, 133.1, 128.0 (maj) and 127.9 (min), 127.3, 126.9, 126.5, 125.4, 125.2, 124.6, 124.4 (min) and 124.3 (maj), 120.2 (min) and 120.1 (maj), 83.3 (min) and 82.5 (maj), 67.4 (maj) and 66.1 (min), 50.0, 49.7 (maj) and 49.5 (min), 47.5 (min) and 47.4 (maj), 40.0 (min) and 39.8 (maj), 34.3, 32.8, 29.6, 28.4 (min) and 28.3 (maj), 26.9, 24.8 ppm. MS (ESI^+): m/z 767.9 $[M + H]^+$, 790.0 $[M + Na]^+$.

*3,4-Bis(tert-butoxycarbonylamino)benzoic Acid (**5**).* To a solution of di-*tert*-butyl dicarbonate (7.20 g, 33.0 mmol) in DMF (15 mL) was added 3,4-diaminobenzoic acid (2.00 g, 13.2 mmol) followed by diisopropylethylamine (2.10 g, 16.0 mmol). The reaction mixture was stirred at room temperature under nitrogen for 16 h and then poured into 150 mL of water. The solution pH was adjusted to 6 using 1 M HCl and extracted with EtOAc (3 × 125 mL). The combined organic layers were washed with water (4 × 50 mL), dried over Na_2SO_4, filtered, and concentrated under reduced pressure. The crude product was recrystallized from chloroform to give **5** as a white solid. Yield: 2.60 g (56%). R_f = 0.25 in 80% EtOAc/hexane. IR (KBr): ν 3367m (N−H), 2981s (C−H_{arom}), 2934m (C−H_{arom}), 1741s (C═O), 1718s (C═O), 1689s (C═O), 1609w, 1499m, 1420m, 1396s, 1369m, 1322s, 1248s, 1160s, 1050m, 1027m, 963w, 876w, 828w, 772m cm^{-1}. ^1H NMR (300 MHz, DMSO-d_6): δ 8.71 (s, 1H), 8.66 (s, 1H), 8.08 (s, 1H), 7.73−7.62 (m, 2H), 1.46 (s, 18H) ppm. ^{13}C NMR (75 MHz, DMSO-d_6): δ 167.6, 154.0, 153.5, 135.2, 129.7, 126.4, 126.1, 125.9, 122.9, 80.8, 80.4, 28.8, 28.7 ppm. MS (ESI^-): m/z 351.2 $[M - H]^-$.

*Ethyl-6-(3,4-bis(tert-butoxycarbonylamino)benzamido)-hexanoate (**6**).* Compound **6** was prepared in a manner similar to **2**, but using 3,4-bis(*tert*-butoxycarbonylamino)benzoic acid (**5**; 0.620 g, 1.75 mmol), Et_3N (0.30 mL, 2.10 mmol), DCC (0.536 g, 2.60 mmol), HOBt (0.311 g, 2.30 mmol), DMAP (25 mg), and ethyl-6-aminohexanoate hydrochloride (0.552 g, 2.82 mmol) in dry DMF (15 mL). The product **6** was isolated as viscous yellow oil. Yield: 0.660 g (76%). R_f = 0.35 in 50% EtOAc/hexane. IR (neat): ν 3365m (N−H), 2979m (C−H_{arom}), 2934m (C−H_{arom}), 2866w (C−H_{aliph}), 1740m (C═O), 1731m (C═O), 1715m (C═O), 1621w, 1518w, 1427m, 1393m, 1368m, 1311w, 1242m, 1159m, 1103w, 1050m, 1027m, 903m, 878w, 826w cm^{-1}. ^1H NMR (300 MHz, $CDCl_3$): δ 7.65 (br s, 1H), 7.54−7.40 (m, 3H), 7.27 (d, ^3J = 7.7 Hz, 1H), 7.106.92 (m, 1H), 4.03 (q, ^3J = 7.1 Hz, 2H), 3.29−3.24 (m, 2H), 2.23−2.19 (m, 2H), 1.571.48 (m, 4H), 1.43 (s, 9H), 1.41 (s, 9H), 1.33−1.28 (m, 2H), 1.16 (t, ^3J = 6.7 Hz, 3H) ppm. ^{13}C NMR (75 MHz, $CDCl_3$): δ 174.0, 167.2, 154.6, 153.8, 134.2, 130.9, 129.2, 124.3, 124.2, 122.8, 81.0, 60.5, 40.1, 34.4, 29.4, 28.5, 26.7, 24.8, 14.5 ppm. MS (ESI^+): m/z 516.1 $[M + Na]^+$.

*Ethyl-6-(3,4-diaminobenzamido)hexanoate (**7**).* Deprotection of ethyl-6-(3,4-bis(*tert*-butoxycarbonylamino)benzamido)hexanoate (**6**; 0.365 g, 0.740 mmol) as for **3** gave **7** as a brown solid. Yield: 0.380 g (98%). IR (neat): ν 3361s (N−H), 3075w (C−H_{arom}), 2932s (C−H_{arom}), 2858m (C−H_{aliph}), 1716s (C═O), 1664s (C═O), 1557w, 1463w, 1456m, 1394w, 1373m, 1323s, 1286w, 1191m, 1158s, 1031m, 973m, 892w, 835m cm^{-1}. ^1H NMR (300 MHz, $CDCl_3$): δ 7.86−7.31 (m, 3H), 6.98 (d, ^3J = 7.7 Hz, 1H), 4.12 (q, ^3J = 7.1 Hz, 2H), 3.463.42 (m, 2H), 2.37−2.30 (m, 2H), 1.661.56 (m, 4H), 1.38−1.34 (m, 2H), 1.20 (t, ^3J = 6.7 Hz, 3H) ppm. ^{13}C NMR (75 MHz, $CDCl_3$): δ 176.5, 168.6, 139.1, 136.4, 134.7, 132.1, 126.8, 120.7, 61.7, 41.1, 34.4, 28.6, 26.2, 24.5, 13.9 ppm. MS (ESI^+): m/z 294.1 $[M + H]^+$.

*6-(Dipyrido[3,2-a:2′,3′-c]phenazine-11-carboxamido)hexanoic Acid (**8**).* 1,10-Phenanthroline-5,6-dione (0.120 g, 0.571 mmol) was heated at reflux in 10 mL of absolute ethanol until dissolution was complete; ethyl-6-(3,4-diaminobenzamido)hexanoate (**7**; 0.387 g, 0.742 mmol) dissolved in ethanol (10 mL) was added and the reaction mixture heated at reflux. Conversion to the product was complete after 5 h of reflux (monitored by TLC). The solvent was evaporated under reduced pressure to obtain the crude product, which was dissolved in 8 mL of MeOH/H_2O (3:1). Solid NaOH (0.100 g, 2.5 mmol) was then added at 0 °C, and after continuous stirring at room temperature for 16 h, the volume was reduced to 4 mL by rotary evaporation. The pH solution was adjusted to pH 3 using 1 M HCl and the suspension cooled overnight at −10 °C to precipitate the product, which was collected by filtration, washed with MeOH, and

air-dried to obtain **8** as a light brown solid. Yield: 0.110 g (43%). IR (KBr): ν 3408m (N−H), 3285s (O−H), 3082w (C−H_{arom}), 3064w (C−H_{arom}), 2928s (C−H_{aliph}), 2860m (C−H_{aliph}), 1718s (C═O), 1689s (C═O), 1638s, 1549m, 1461w, 1419m, 1405m, 1389m, 1377w, 1363m, 1218m, 1191m, 1169w, 1129w, 1072s, 1032m, 892m, 819m, 741s cm^{-1}. ^1H NMR (300 MHz, DMSO-d_6): δ 9.44−9.39 (m, 2H), 9.18 (dd, ^3J = 4.2 Hz, ^4J = 1.5 Hz, 2H), 8.96 (t, ^3J = 5.6 Hz, 1H), 8.76 (br s, 1H), 8.38−8.31 (m, 2H), 7.90−7.87 (m, 2H), 2.26 (t, ^3J = 7.2 Hz, 2H), 1.66−1.56 (m, 4H), 1.451.39 (m, 2H) ppm. Two proton signals are masked by residual water from DMSO-d_6. ^{13}C NMR (75 MHz, DMSO-d_6): δ 175.0, 165.5, 153.0, 152.9, 148.4, 148.3, 142.9, 142.0, 141.8, 141.4, 136.8, 133.6, 133.3, 129.9, 129.6, 128.4, 127.1, 125.0, 124.9, 39.9, 34.2, 29.2, 26.6, 24.8 ppm. MS (ESI^-): m/z 438.1 $[M - H]^-$.

*tert-Butyl-2-(N-(2-(((9H-fluoren-9-yl)methoxy)carbonylamino)-ethyl)-6-(dipyrido[3,2-a:2′,3′-c]phenazine-11-carboxamido)-hexanamido)acetate (**dppz-L-PNA**).* 6-(Dipyrido[3,2-*a*:2′,3′-*c*]-phenazine-11-carboxamido)hexanoic acid (**8**; 0.068 g, 0.150 mmol) was suspended in dry DMF (5 mL) under nitrogen. HBTU (0.095 g, 0.250 mmol) and DMAP (0.020 g) were added to the suspension, and the reaction mixture was stirred at room temperature for 30 min. *tert*-Butyl-2-(2-(((9H-fluoren-9-yl)methoxy)carbonylamino)ethylamino)-acetate hydrochloride (0.108 g, 0.250 mmol) was then added and stirring continued for a further 15 min. The reaction mixture was cooled to 0 °C, and diisopropylethylamine (40.0 μL, 0.250 mmol) was then added dropwise. After stirring, the mixture at 0 °C for 30 min, it was stirred at room temperature for a further 18 h. Water (10 mL) and DCM (25 mL) were added and the mixture stirred for 2 h. The organic layer was separated, and the aqueous layer was further extracted with DCM (2 × 15 mL). The DCM layers were combined, dried over Na_2SO_4, filtered, and concentrated to obtain the crude product, which was purified by column chromatography (SiO_2, eluent polarity gradually changed from 100% EtOAc to 10% MeOH/DCM) to afford **dppz-L-PNA** as a yellow solid. Yield: 0.101 g (80%). R_f = 0.40 in 10% MeOH/DCM. IR (KBr): ν 3068w (C−H_{arom}), 3014w (C−H_{arom}), 2930s (C−H_{aliph}), 2865m (C−H_{aliph}), 1734s (C═O), 1718s (C═O), 1687m (C═O), 1642s, 1539m, 1461m, 1407m, 1390w, 1365m, 1250m, 1155s, 1074m, 1035m, 847s, 760w, 741m cm^{-1}. ^1H NMR (400 MHz, DMSO-d_6): mixture of rotamers δ 9.17−9.06 (m, 4H), 8.88 (m, 1H), 8.57 (m, 1H), 8.28−8.26 (rotamers, m, 1H), 8.10 (t, ^3J = 8.0 Hz, 1H), 7.83−7.74 (rotamers, m, 4H), 7.64−7.58 (rotamers, m, 2H), 7.38−7.21 (m, 4H), 4.30−4.26 (m, 2H), 4.18−4.10 (m, 2H), 3.91 (m, 1H), 3.20−3.11 (rotamers, m, 2H), 2.41−2.21 (m, 2H), 1.66−1.59 (m, 4H), 1.44−1.39 (m, 11H) ppm. Four proton signals are masked by residual water from DMSO-d_6. ^{13}C NMR (100 MHz, DMSO-d_6): mixture of rotamers δ 173.4 (min) and 173.0 (maj), 173.8, 169.6 (min) and 169.1 (maj), 165.4, 156.7 (maj) and 156.6 (min), 152.8, 152.7, 148.0, 147.9, 144.3, 144.2, 143.0, 142.6, 141.5, 141.3, 141.1, 139.8, 137.8, 136.6, 133.5, 133.1, 129.7, 129.4, 129.3, 128.3, 128.0 (min) and 127.9 (maj), 127.7, 127.4, 126.9, 125.5, 125.4, 124.8, 121.8, 120.5, 120.4, 81.9 (min) and 81.0 (maj), 65.9, 51.2, 49.1 (maj) and 48.8 (min), 47.2, 39.9, 38.9, 32.6 (maj) and 32.2 (min), 29.3, 28.2 (maj) and 28.1 (min), 26.7, 24.8 ppm. MS (ESI^+): m/z 818.4 $[M + H]^+$.

*[Ru(bpy)$_2$(dpq-L-PNA−OH)](PF$_6$)$_2$·1.5H$_2$O (**M1**).* dpq-L-PNA (0.120 g, 0.16 mmol) was stirred in a 1:1 solution of TFA/CH_2Cl_2 (5 mL), at room temperature for 5 h. The solvent was evaporated under reduced pressure to yield an oily residue, which was triturated with toluene, $CHCl_3$, and ether. The yellow solid obtained was dissolved in degassed EtOH/H_2O solution (1:1, 8 mL), $Ru(bpy)_2Cl_2$ (0.058 g, 0.12 mmol) added, and the solution refluxed under a N_2 atmosphere for 4.5 h. The solvent was removed under reduced pressure, and the residue was diluted with water (10 mL) and filtered. An aqueous solution of HPF_6 (60%) was then added dropwise to the filtrate, until no further precipitation was observed. The orange precipitate was collected by filtration, dissolved in acetonitrile, reprecipitated by the addition of diethylether, filtered, and dried under high vacuum conditions to give **M1** as an orange powder. Yield: 0.111 g (66%). Anal. Calcd for $C_{60}H_{56}F_{12}N_{11}O_{7.5}P_2Ru$ (%): C, 49.97; H, 3.91; N, 10.68. Found: C, 49.89; H, 3.74; N, 10.76. IR (KBr): ν 3425br (O−H), 3081m (C−H_{arom}), 3067w (C−H_{arom}), 2930m (C−H_{aliph}), 2857w (C−H_{aliph}), 1703s (C═O), 1653s (C═O), 1544w, 1446m, 1414m, 1390w, 1373w, 1244m, 1164m, 1121m, 1082w, 1051w, 1020w, 843vs, 763s, 741m, 730s cm^{-1}. ^1H NMR (400 MHz, acetone-d_6): mixture of rotamers δ 9.88−9.72 (rotamers, m, 1H), 9.54 (s, 1H), 9.52−9.47 (m, 1H), 9.02−8.96 (min) and 8.84−8.78 (maj) (rotamers, m, 4H), 8.57−8.49 (m, 2H), 8.24−8.21 (m, 2H), 8.16−8.14 (m, 4H), 8.08−7.98 (m, 5H), 7.727.70 (m, 1H), 7.63−7.48 (m, 5H), 7.42−7.37 (m, 2H), 7.30−7.17 (rotamers, m, 4H), 4.20−4.18 (m, 2H), 4.12 (q, ^3J = 7.4 Hz, 1H), 4.06−3.98 (m, 2H), 3.59−3.30 (m, 6H), 2.41−2.25 (m, 2H), 1.60−1.56 (m, 4H), 1.41−1.33 (m, 2H) ppm. MS (ESI^+): m/z 562.4 $[M]^{2+}$.

*[Ru(phen)$_2$(dpq-L-PNA−OH)](PF$_6$)$_2$·4H$_2$O (**M2**).* Complex **M2** was obtained as an orange solid employing the procedure described for **M1**, using dpq-L-PNA (0.120 g, 0.16 mmol) and $Ru(phen)_2Cl_2$ (0.053 g, 0.10 mmol) in EtOH/H_2O (1:1, 8 mL). Yield: 0.094 g (60%). Anal. Calcd for $C_{64}H_{61}F_{12}N_{11}O_{10}P_2Ru$ (%): C, 50.07; H, 4.00; N, 10.04. Found: C, 50.02; H, 3.86; N, 10.20. IR (KBr): ν 3450br (O−H), 3085w (C−H_{arom}), 3063w (C−H_{arom}), 2928s (C−H_{aliph}), 2856m (C−H_{aliph}), 1707m (C═O), 1650s (C═O), 1637s, 1542w, 1445m, 1428m, 1407m, 1227w, 1165m, 1056w, 841vs, 763m, 742m, 723s cm^{-1}. ^1H NMR (400 MHz, acetone-d_6): mixture of rotamers δ 9.79−9.73 (rotamers, m, 1H), 9.659.53 (m, 1H), 8.82−8.75 (m, 4H), 8.628.51 (rotamers, m, 2H), 8.50−8.48 (m, 1H), 8.43−8.38 (m, 7H), 8.32−8.27 (m, 1H), 7.99−7.92 (m, 1H), 7.87−7.73 (m, 6H), 7.69−7.45 (m, 4H), 7.34−7.21 (m, 2H), 7.19−7.17 (m, 2H), 4.27−4.24 (m, 2H), 4.15 (q, ^3J = 7.4 Hz, 1H), 4.07−4.04 (m, 2H), 3.58−3.48 (m, 4H), 3.39−3.34 (maj) and 3.25−3.24 (min) (rotamers, m, 2H), 2.46−2.43 (maj) and 2.33−2.30 (min) (rotamers, m, 2H), 1.73−1.64 (m, 4H), 1.51−1.42 (m, 2H) ppm. MS (ESI^+): m/z 586.4 $[M]^{2+}$.

*[Ru(bpy)$_2$(dppz-L-PNA−OH)](PF$_6$)$_2$·2.5H$_2$O (**M3**).* Complex **M3** was synthesized by means analogous to those used for preparation of **M1**, using dppz-L-PNA (0.082 g, 0.10 mmol) and $Ru(bpy)_2Cl_2$ (0.039 g, 0.08 mmol) in EtOH/H_2O (1:1, 6 mL). The desired complex was isolated as an orange solid. Yield: 0.075 g (62%). Anal. Calcd for $C_{64}H_{60}F_{12}N_{11}O_{8.5}P_2Ru$ (%): C, 50.90; H, 4.00; N, 10.20. Found: C, 50.73; H, 3.81; N, 10.42. IR (KBr): ν 3425br (O−H), 3075w (C−H_{arom}), 2931s (C−H_{aliph}), 2862m (C−H_{aliph}), 1720s (C═O), 1706s (C═O), 1638m, 1535m, 1463m, 1447m, 1408w, 1358w, 1245m, 1184w, 1121w, 1079m, 1048w, 949w, 844vs, 763s, 741m, 730m cm^{-1}. ^1H NMR (400 MHz, acetone-d_6): mixture of rotamers δ 9.64−9.61 (min) and 9.58−9.48 (maj) (rotamers, m, 2H), 8.86−8.80 (m, 4H), 8.58−8.50 (m, 3H), 8.26−8.21 (m, 4H), 8.18−8.12 (m, 6H), 8.05−7.98 (m, 2H), 7.71−7.61 (rotamers, m, 3H), 7.57−7.55 (m, 2H), 7.53−7.49 (m, 2H), 7.47−7.42 (m, 2H), 7.27 (t, ^3J = 7.4 Hz, 1H), 7.21−7.12 (rotamers, m, 3H), 4.30−4.22 (m, 2H), 4.21−4.15 (rotamers, m, 2H), 4.09 (q, ^3J = 7.4 Hz, 1H), 3.61−3.55 (m, 2H), 3.43−3.38 (m, 2H), 3.30−3.25 (m, 2H), 2.49−2.31 (m, 2H), 1.66−1.56 (m, 4H), 1.44−1.38 (m, 2H) ppm. m/z 587.7 $[M]^{2+}$.

*[Ru(phen)$_2$(dppz-L-PNA−OH)](PF$_6$)$_2$·2.5H$_2$O (**M4**).* Using the method described for the synthesis of **M1**, $[Ru(phen)_2$(dppz-L-PNA−OH)$](PF_6)_2$ was prepared from dppz-L-PNA (0.197 g, 0.26 mmol) and $Ru(phen)_2Cl_2$ (0.111 g, 0.21 mmol). This afforded **M4** as an orange powder. Yield: 0.174 g (55%). Anal. Calcd for $C_{68}H_{60}F_{12}N_{11}O_{8.5}P_2Ru$ (%): C, 52.41; H, 3.88; N, 9.89. Found: C, 52.37; H, 3.65; N, 9.90. IR (KBr): ν 3448br (O−H), 3065w (C−H_{arom}), 2929s (C−H_{aliph}), 2864m (C−H_{aliph}), 1720s (C═O), 1701s (C═O), 1651m (C═O), 1560w, 1544m, 1445w, 1428m, 1410m, 1239w, 1145m, 1108w, 1079m, 1054w, 841vs, 775m, 762m, 742m, 723s cm^{-1}. ^1H NMR (300 MHz, CD_3CN): mixture of rotamers δ 9.56−9.53 (m, 1H), 9.52−9.44 (m, 1H), 8.75−8.71 (m, 4H), 8.64−8.58 (m, 1H), 8.43−8.36 (rotamers, m, 6H), 8.27−8.25 (m, 2H), 8.24−8.17 (m, 2H), 8.16−8.12 (m, 2H), 7.85−7.80 (m, 3H), 7.79−7.76 (m, 2H), 7.75−7.66 (rotamers, m, 3H), 7.50−7.45 (rotamers, m, 3H), 7.32−7.20 (m, 1H), 7.17−7.10 (m, 3H), 4.30−4.21 (romaters, m, 2H), 4.13−4.08 (m, 3H), 3.57−3.51 (m, 2H), 3.37−3.27 (m, 4H), 2.35−2.21 (rotamers, m, 2H), 1.73−1.59 (m, 4H), 1.49−1.40 (m, 2H) ppm. MS (ESI^+): m/z 611.7 $[M]^{2+}$.

dx.doi.org/10.1021/ic201911f | *Inorg. Chem.* 2011, 50, 12172−12183

Scheme 1. Synthesis of M1 and M2[a]

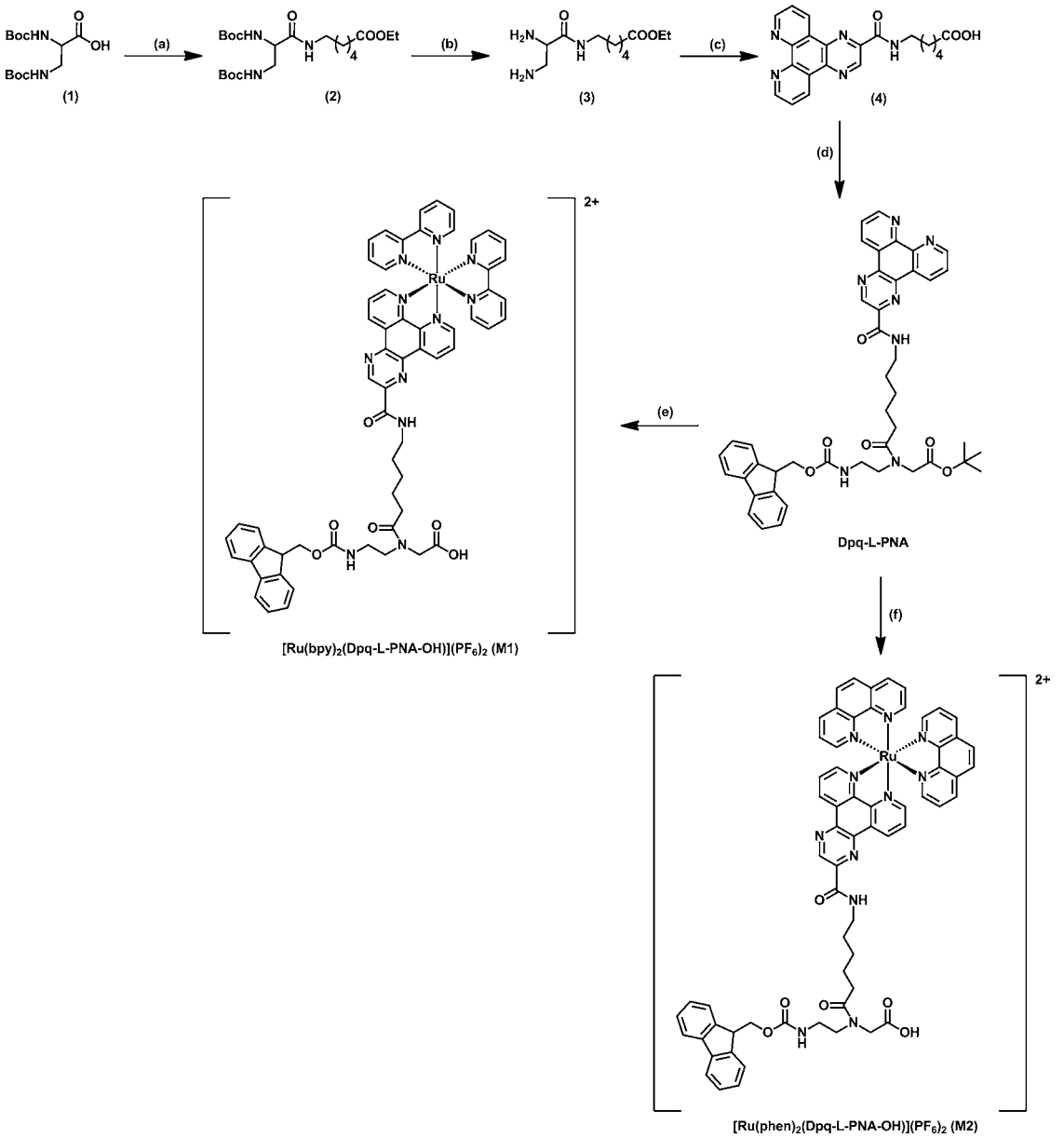

[a]Reagents and conditions: (a) ethyl-6-aminohexanoate hydrochloride, HOBt, DCC, DMAP, Et_3N, dry THF, rt, 16 h, 75%. (b) TFA/CH_2Cl_2 (1:1), rt, 5 h, 98%. (c) **1**: 1,10-phenanthroline-5,6-dione, EtOH, Δ, 5 h. **2**: NaOH, MeOH/H_2O (3:1), 0 °C–rt, 16 h, 63%. (d) *tert*-butyl *N*-[2-(*N*-9-fluorenylmethoxycarbonyl)-aminoethyl]glycinate, HBTU, Et_3N, dry DMF, DIPEA, rt, 18 h, 73%; (e) **1**: TFA/CH_2Cl_2 (1:1), rt, 5 h. **2**: $Ru(bpy)_2Cl_2$, EtOH/H_2O (1:1), Δ, 4.5 h, 66%; (f) **1**: TFA/CH_2Cl_2 (1:1), rt, 5 h. **2**: $Ru(phen)_2Cl_2$, EtOH/H_2O (1:1), Δ, 4.5 h, 60%.

RESULTS AND DISCUSSION

Synthesis. The synthesis of the Ru(II)–PNA monomers **M1**, **M2**, **M3**, and **M4**, described in detail in Schemes 1 and 2, followed a similar approach to that reported by Achim et al.[21] involving the preparation of the bipyridine-modified PNAs, which were then incorporated into Ru(II) complexes by reaction with either $[Ru(bpy)_2Cl_2]$ or $[Ru(phen)_2Cl_2]$. The metal chelating scaffolds, dpq-L-PNA and dppz-L-PNA, were first prepared by reacting the respective carboxamido derivatives, **3** and **7**, with 1,10-phenanthroline-5,6-dione, *in situ* base mediated hydrolysis to form the dipyridoquinoxaline (dpq) and dipyridophenazine (dppz) carboxylic acid derivatives, **4** and **8**, and their subsequent coupling to the protected aminoethyl-glycine-based PNA monomer backbone. The PNA–monomer esters, dpq-L-PNA and dppz-L-PNA, and the intermediate derivatives were characterized using ^1H and ^{13}C NMR spectroscopy, IR spectroscopy, and ESI-MS. In the ^1H NMR spectra for **4** and **8**, peak integration in the aromatic region (7.00–9.00 ppm) corresponding to 8*H* and 10*H*, respectively, along with the disappearance of upfield proton signals between 4.00 and 4.20 ppm and 1.13–1.24 ppm confirmed the hydrolysis of the ester. The IR spectrum of **4** and **8** showed two CO stretching vibrations between 1720 cm^{-1} and 1670 cm^{-1}, assigned to amide and carboxylic acid functionalities. $[M - H]^-$ peaks at m/z = 388.0 (**4**) and 438.1 (**8**) in the ESI-MS further confirmed the formation of the products. The identity of the modified PNA monomer esters, dpq-L-PNA and dppz-L-PNA, obtained in good yields (73–

dx.doi.org/10.1021/ic201911f | *Inorg. Chem.* 2011, 50, 12172–12183

Scheme 2. Synthesis of M3 and M4[a]

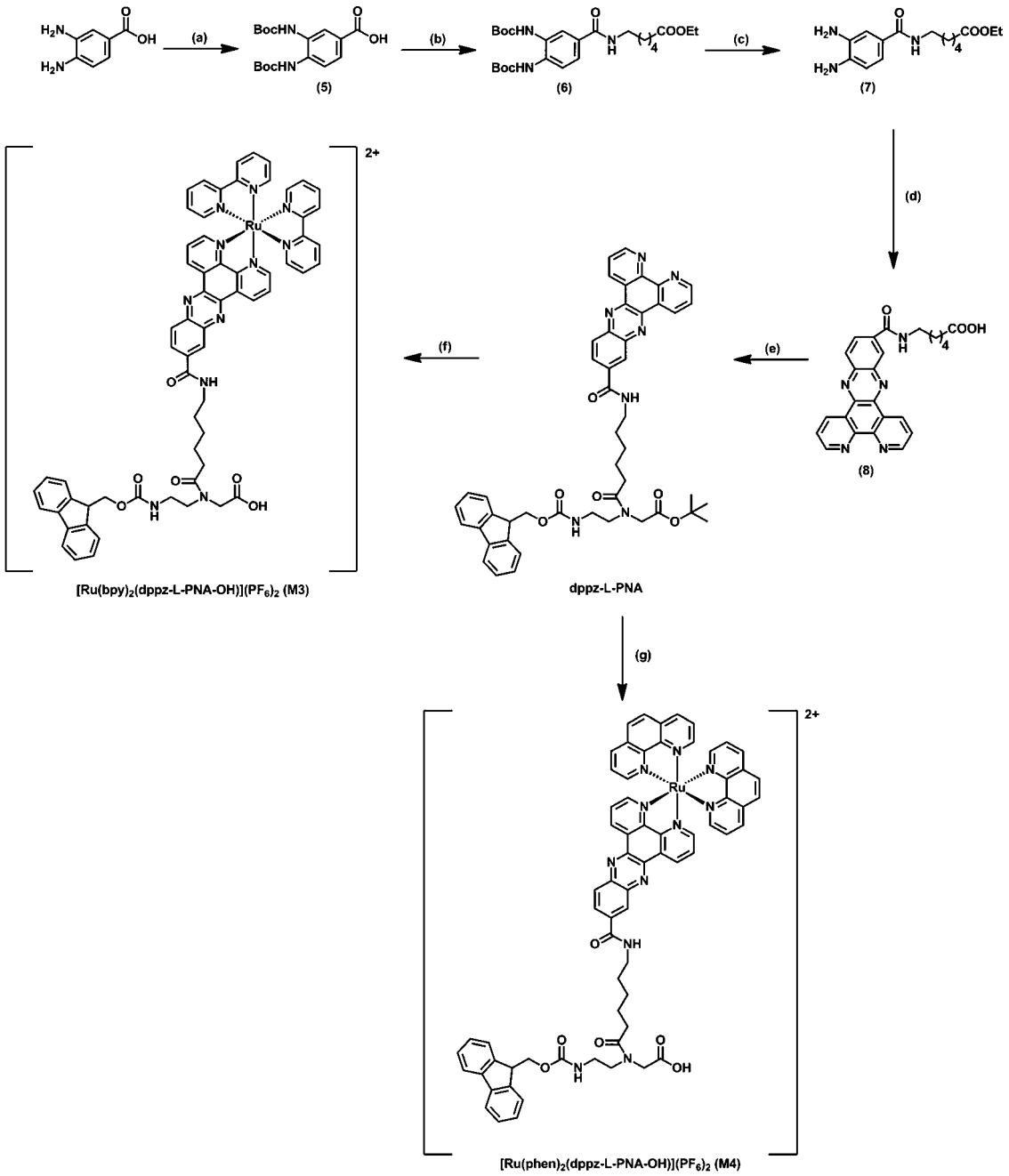

[a]Reagents and conditions: (a) di-*tert*-butyl dicarbonate, DIPEA, DMF, rt, 16 h, 56%. (b) ethyl-6-aminohexanoate hydrochloride, HOBt, DCC, DMAP, Et_3N, dry DMF, rt, 16 h, 76%. (c) TFA/CH_2Cl_2 (1:1), rt, 5 h, 98%. (d) **1**: 1,10-phenanthroline-5,6-dione, EtOH, Δ, 5 h. **2**: NaOH, MeOH/H_2O (3:1), 0 °C−rt, 16 h, 43%. (e) *tert*-butyl *N*-[2-(*N*-9-fluorenylmethoxycarbonyl)aminoethyl]glycinate, HBTU, Et_3N, dry DMF, DIPEA, rt, 18 h, 80%. (f) **1**: TFA/CH_2Cl_2 (1:1), rt, 5 h. **2**: $Ru(bpy)_2Cl_2$, EtOH/H_2O (1:1), Δ, 4.5 h, 62%. (g) **1**: TFA/CH_2Cl_2 (1:1), rt, 5 h. **2**: $Ru(phen)_2Cl_2$, EtOH/H_2O (1:1), Δ, 4.5 h, 55%.

80%), was confirmed by ESI-MS, which showed peaks at m/z = 767.9 (dpq-L-PNA) and 818.4 (dppz-L-PNA) corresponding to the $[M + H]^+$ ions. The ^1H NMR spectrum of the monomers exhibited the expected signals due to the Fmoc and the *tert*-butyl group in addition to resonances similar to those found for the carboxylic acid precursors, **4** and **8**. The IR spectrum showed overlapping CO stretching vibrations due to ester and amide functionalities (1655−1703 cm^{-1}) as well as aromatic C−H (3014−3068 cm^{-1}) and aliphatic C−H (2856−2930 cm^{-1}) stretches.

The Ru(II)−bis(bipyridyl) complexes, **M1** and **M3**, were prepared by reaction of the boc-deprotected dpq-L-PNA and dppz-L-PNA monomers with $Ru(bpy)_2Cl_2$ and isolated as hexafluorophosphate salts. Similar reactions of dpq-L-PNA and dppz-L-PNA with $Ru(phen)_2Cl_2$ gave the complexes **M2** and **M4**, respectively. The Ru(II)-based PNA monomers were isolated as a rotameric mixture in reasonable yields (55−70%) and in high purity with no further chromatographic purification required. Signals at m/z values of 562.4 (**M1**), 586.4 (**M2**), 587.7 (**M3**), and 611.7 (**M4**) for the corresponding $[M]^{2+}$ ion

dx.doi.org/10.1021/ic201911f | *Inorg. Chem.* 2011, 50, 12172−12183

observed in ESI-MS and elemental analysis confirmed the successful synthesis of the target complexes. Coordination of the dipyridoquinoxaline and dipyridophenazine units to the Ru(II) center was established by comparison of the ^{1}H NMR spectra of the free ligand and complexes. The ^{1}H NMR spectra of complexes **M1**−**M4** showed additional aromatic signals for the introduced bipyridine and phenanthroline moieties. The disappearance of the singlet between 1.50 and 1.39 ppm for the *tert*-butyl CH_3 groups confirmed the hydrolysis of the *t*-boc functionality in the parent ligand. As expected, the IR spectrum retained overlapping CO stretching vibrations for the carbonyl stretching vibration in ester and amide functionalities (1650−1703 cm^{-1}) as well as aromatic C−H (3063−3085 cm^{-1}) and aliphatic C−H (2856−2930 cm^{-1}) stretches. Thus, the spectroscopic data indicate that the modular approach employed to prepare **M1**−**M4** successfully overcomes the previously described problems of purity and isolation of similar Ru(II)−polypyridyl complexes attached onto the PNA monomeric backbone.[37] In addition, the monomeric PNA scaffolds, dpq-L-PNA and dppz-L-PNA, can be conveniently used to prepare libraries of transition metal−PNA monomers and oligomeric PNA scaffolds for transition metal ions.

Electronic Absorption Spectra. The UV−visible spectra of **M1**−**M4**, measured in acetonitrile at (10 ± 1) μM, are as shown in Figure 2, and the spectral data are summarized in Table 1. Complexes **M1**−**M4** are classical Ru(II) complexes of the form $[Ru(L)_2L']^{2+}$, where L and L′ are both polypyridyl ligands. As for related complexes,[37,42,48,67−69] the absorption spectra for **M1**−**M4** exhibit broad overlapping MLCT (metal to ligand charge transfer) bands at ca. 450 nm due to dπ−π* transitions from Ru(II) center into the mixed π* orbitals of the ligands (L(π*) and L′(π*)). More intense absorption bands ascribable to the intraligand π−π* transitions are observed between 250 and 300 nm in each case. Characteristic π−π* transitions localized on the dppz ligand are also in seen in the spectra of **M3** and **M4** at 372 and 375 nm, respectively. The energy and intensity of the associated transition bands depend on ligand L′ (dppz or dpq), giving rise to subtle differences in the absorption maxima for the phenanthroline complexes, **M2** and **M4**, compared with the bipyridyl complexes, **M1** and **M3**.

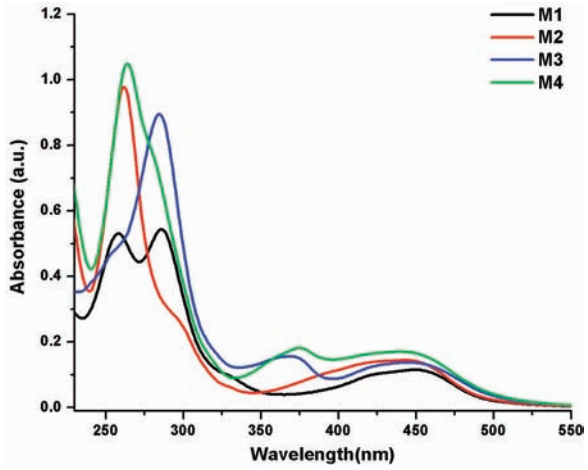

Figure 2. Absorption spectra for **M1**−**M4** (10 ± 1 μM) measured in acetonitrile.

Table 1. UV−Vis Spectroscopic Data Obtained for 10 ± 1 μM Acetonitrile Solutions of M1−M4

complex	λ_{max} (nm) [LC]	ε_{molar} (M^{-1} cm^{-1})	λ_{max} (nm) [MLCT]	ε_{molar} (M^{-1} cm^{-1})
M1	258	53100	421	10100
	283	55400	453	11700
M2	262	97800	443	14000
	298	26700		
M3	254	46900	448	14300
	284	89300		
	372	15600		
M4	264	105000	449	17000
	280	77900		
	375	18200		

Photoluminescence Spectroscopy. Steady state emission spectra for 10 ± 1 μM acetonitrile solutions of **M1**−**M4** were recorded with excitation of the MLCT band at 450 nm (Figure 3). The profiles are consistent with the ^{3}MLCT emission commonly observed in Ru(II) polypyridyl complexes.[42] As listed in Table 2, the Ru(II) dpq complexes, **M1** and **M2**, exhibit emission maxima at 618 and 613 nm, respectively, similar to the $[Ru(bpy)_3]^{2+}$ emission wavelength (615 nm). On the contrary, dppz-based Ru(II)−PNA monomers, **M3** and **M4**, show a red shift in their emission maxima to 658 and 660 nm, respectively. The integrated emission intensities, measured as the total number of emitted photons between 500 and 800 nm, showed that the dpq complex, **M1**, has a similar emission efficiency to that of the dppz derivatives (**M3** and **M4**), while that for **M2** was slightly lower (Table 2). The differences in the emission maxima indicate significant influence from the dpq and dppz ligands on the HOMO and/or LUMO energy levels. The relative

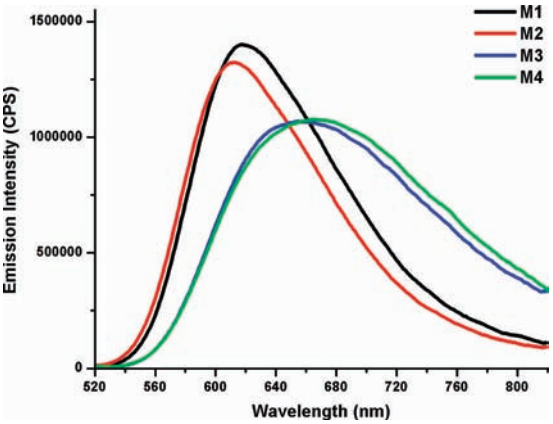

Figure 3. Photoluminescence emission spectra recorded on excitation of 10 ± 1 μM acetonitrile solutions of **M1**−**M4** at 450 nm.

Table 2. Summary of Emission Spectral Data Measured for M1−M4 (10 ± 1 μM Solutions in Acetonitrile) Following Excitation at 450 nm

complex	λ_{max} (nm)	I_s/I_{ref} (CH_3CN)	Φ_R
M1	618	1.18	0.078
M2	613	1.08	0.058
M3	658	1.21	0.068
M4	660	1.23	0.057
$[Ru(bpy)_3]^{2+}$ [68]	615	1.00	0.062

dx.doi.org/10.1021/ic201911f | *Inorg. Chem.* 2011, 50, 12172−12183

positioning of the emission maxima (**M1** and **M2** vs **M3** and **M4**) suggests low-lying LUMO levels in the dppz complexes, relative to $[Ru(bpy)_3]^{2+}$ or the dpq complexes.

The emission quantum yields (Φ_R) for **M1**−**M4** (Table 2) were determined assuming Φ_{ref} for $[Ru(bpy)]^{3+}$ to be 0.062 and using the equation:

$$\Phi_R = \Phi_{ref}(I_s A_{ref})/(I_{ref} A_s)$$

where I_s and I_{ref} are the integrated emission intensities calculated from the area under the emission spectrum of the sample and reference, respectively, and A_s and A_{ref} are the absorbances of the sample and reference, respectively.[48,67]

The quantum yield for **M1** was slightly higher than for the reference compound, $[Ru(bpy)_3]^{2+}$, whereas it was similar for **M2**, **M3**, and **M4**. In general, the bis(bipyridyl) Ru(II) complexes, **M1** and **M3**, showed higher quantum yields than the bis(phenanthroline) derivatives, **M2** and **M4**. However, no such differentiation based on ancillary ligands in the Ru(II) coordination sphere could be made in the relative emission intensities and the emission maxima for the complexes (*vide supra*).

Electrochemistry. Cyclic voltammograms for the oxidation of complexes **M1**−**M4** recorded in acetonitrile at a scan rate of 100 mV s^{-1} are presented in Figure 4.

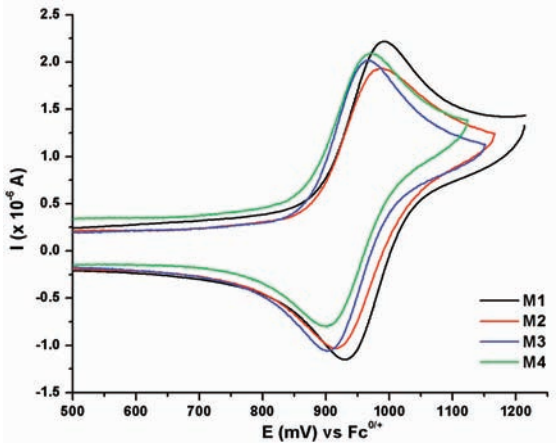

Figure 4. Cyclic voltammograms obtained at a glassy carbon electrode using a scan rate of 100 mV s^{-1} for the oxidation of 1 mM Ru(II) complexes in CH_3CN (0.1 M nBu_4NPF_6).

All complexes exhibited a single essentially reversible oxidation process associated with the Ru^{II}/Ru^{III} couple. The formal potentials ($E_f^\circ = E_m$) for the one electron oxidation process, calculated over the scan rate range of 100−1000 mV s^{-1} by averaging the oxidation and reduction peak potentials to give the midpoint potential E_m, are given in Table 3 (with representative voltammograms shown in Figures S5−S8, Supporting Information). The E_f° values determined for **M1**−**M4** were 962, 951, 936, and 938 mV, respectively, vs $Fc^{0/+}$. Relative to the E_f° values for the $[Ru(bpy)_3]^{2+}/[Ru(bpy)_3]^{3+}$ system (888 mV vs $Fc^{0/+}$),[68] this indicates a positive shift in potential for the Ru(II)−PNA monomers **M1**−**M4** of up to 74 mV. The electrochemical data in conjunction with the emission profile of the complex can be used to probe changes in molecular orbital levels. The small blue shift of the emission maxima and a relatively positive reversible potential indicate stabilization of the HOMO in **M1** and **M2** and widening of the HOMO−LUMO gap for the emission process compared with $[Ru(bpy)_3]^{2+}$. On the other hand, the red shifts in emission observed for **M3** and **M4** may be rationalized by a relatively greater stabilization of the dppz-localized π^* LUMO energy levels compared to the small stabilization of the HOMO indicated by the positive shift in E_m relative to $[Ru(bpy)_3]^{2+}$.

The very small changes in E_m for the $Ru^{2+/3+}$ couple observed on changing dpq to dppz (**M3**−**M1** = 26 mV, **M4**−**M2** = 13 mV) suggests that the energy of the HOMO is relatively unaffected by the introduction of the phenyl ring. This means that the emission spectra for the two dppz complexes, **M3** and **M4**, are red-shifted as a result of stabilization of the LUMO. However, this direct correlation between the photophysical and electrochemical properties can only be validated by studying the ligand-based reduction process for the HOMO−LUMO gap. Unfortunately, the ligand-based reduction steps are not simple reversible processes, so the required thermodynamic data are not available.

The diffusion controlled nature of the oxidation process was confirmed by the linear dependence of the oxidation peak current (i_p^{ox}) on the square root of the scan rate (ν). The diffusion coefficients calculated from the slope of these linear plots and use of the Randles−Sevcik relationship[71−73] are **M1** $(1.89 \pm 0.1) \times 10^{-5}$ cm^2 s^{-1}; **M2** $(1.18 \pm 0.1) \times 10^{-5}$ cm^2 s^{-1}; **M3** $(1.35 \pm 0.1) \times 10^{-5}$ cm^2 s^{-1}; and **M4** $(1.34 \pm 0.1) \times 10^{-5}$ cm^2 s^{-1}. The values are comparable to those reported for other Ru(II) polypyridyl complexes as well as their PNA−monomer derivatives.[37,68]

Electrochemiluminescence. The ECL properties of **M1**−**M4** in acetonitrile with 0.1 M tripropylamine (TPA) as a coreactant were investigated. To the best of our knowledge, the potential of Ru(II)−PNA-like monomers as the basis for ECL biosensors remains unexplored. No studies appear to have been reported on the ECL of such compounds or, for that matter, any other PNA-based conjugates. Low complex concentrations and high coreactant levels were chosen for the ECL experiments, which provide relevance to practical biosensing applications of these Ru(II)−PNA-like monomers. The measured ECL emission intensities were as illustrated in Figure 5. Emission maxima for **M1**−**M4** were 622, 616, 673, and 675 nm, respectively. No ECL signal was detected in similar experiments using only the PNA backbone itself, indicating that it does not interfere with these measurements. The oxidation−reduction mode of coreactant ECL for $[Ru(L)_3]^{2+}$ and tripropylamine (TPA) is mechanistically described in eqs 1−5:[74−77]

$$[Ru(L)_3]^{2+} \rightleftharpoons [Ru(L)_3]^{3+} + e^- \quad (1)$$

$$N(C_3H_7)_3 \rightleftharpoons N(C_3H_7)_3^{\bullet+} + e^- \quad (2)$$

$$N(C_3H_7)_3^{\bullet+} \rightleftharpoons CH_3CH_2C^{\bullet}HN(C_3H_7)_2 + H^+ \quad (3)$$

$$CH_3CH_2C^{\bullet}HN(C_3H_7)_2 + [Ru(L)_3]^{3+} \rightleftharpoons [Ru(L)_3]^{2+*} + P \quad (4)$$

$$[Ru(L)_3]^{2+*} \rightleftharpoons [Ru(L)_3]^{2+} + h\nu \quad (5)$$

However, it should be noted that the oxidation of the amine described in reaction2 may also occur via homogeneous reaction with $[Ru(L)_3]^{3+}$.[74−76]

Figure 5 compares the ECL spectra for the four complexes with that of the $[Ru(bpy)_3]^{2+}$ standard. That the ECL emission maxima (622, 616, 673, and 675 nm for **M1**−**M4**) were

dx.doi.org/10.1021/ic201911f | Inorg. Chem. 2011, 50, 12172−12183

Table 3. Cyclic Voltammetric Data Obtained As a Function of Scan Rate (ν) at a Glassy Carbon Electrode As Derived from Oxidation of 1.0 mM CH_3CN Solutions of M1−M4 in CH_3CN (0.1 M nBu$_4$NPF$_6$) at (20 ± 2) °C

complex	ν (mV s^{-1})	E_p^{ox} (mV)[a,b]	E_p^{red}(mV)[a,b]	ΔE_p (mV)[a,b]	E_m (mV)[a,b]	$\lvert i_p^{ox}/i_p^{red}\rvert$[a,c]
M1	100	988	935	53	962	0.91
	200	990	932	58	961	0.93
	300	992	932	60	962	0.94
	400	996	934	62	965	0.93
	500	996	932	64	964	0.94
	700	996	932	64	964	0.94
	1000	998	934	64	966	0.93
M2	100	983	918	65	951	0.93
	200	986	918	68	952	0.94
	300	986	916	70	951	0.94
	400	986	916	70	951	0.94
	500	986	919	67	953	0.94
	700	988	916	72	952	0.94
	1000	988	918	70	953	0.93
M3	100	966	905	61	936	0.88
	200	966	907	59	937	0.89
	300	966	905	61	936	0.90
	400	966	905	61	936	0.90
	500	966	905	61	936	0.91
	700	968	903	65	936	0.91
	1000	970	903	67	937	0.90
M4	100	970	906	64	938	0.78
	200	973	906	67	940	0.78
	300	973	906	67	940	0.81
	400	973	906	67	940	0.81
	500	974	906	68	940	0.80
	700	978	906	72	942	0.81
	1000	978	903	75	941	0.82

[a]Oxidation peak potential = E_p^{ox}; reduction peak potential = E_p^{red}; midpoint potential = $E_m = (E_p^{ox} + E_p^{red})/2$ versus $Fc^{0/+}$; oxidation peak current = i_p^{ox}; reduction peak current = i_p^{red}. [b]Peak potentials have an error of ±5 mV versus $Fc^{0/+}$. [c]The ratios of peak currents associated with the oxidation and reduction peak currents were calculated according to the empirical method derived by Nicholson.[70]

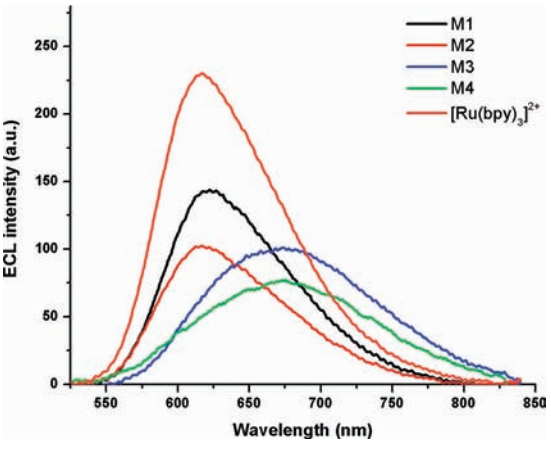

Figure 5. ECL spectra for Ru(II)−PNA monomers and $[Ru(bpy)_3]^{2+}$ in acetonitrile (0.1 M nBu$_4$NPF$_6$). The ECL was generated using a 3 mm diameter glassy carbon electrode with 0.1 mM **M1**−**M3** and $[Ru(bpy)_3]^{2+}$ or 0.2 mM **M4**, containing 0.1 M TPA as a coreactant.

observed at slightly longer wavelengths compared with the photoluminescence (PL) in each case may be simply explained by considering the different detectors used, i.e., a PMT for PL and a CCD for ECL. The ECL λ_{max} data may be regarded as closer to the true values because of the relatively small variation in responsivity with wavelength associated with CCD detectors.[78] Under the conditions described above, the integrated intensities for ECL generated from the PNA monomers follow the order **M1** (62%) ≥ **M3** (60%) > **M4** (46%) ≥ **M2** (44%). The ECL intensities for the complexes are only moderately lower than that of $[Ru(bpy)_3]^{2+}$, which may be regarded as the benchmark ECL emitter. These data suggest that the complexes are promising candidates for ECL-based biosensing applications.

ECL intensities are governed by the ECL efficiency, Φ_{ECL} (photons emitted per electron transferred in reaction 4 above), which is strictly limited by the quantum yield, Φ_R. Therefore, a correlation might be expected between ECL intensity and quantum yield. That such a correlation was not observed in this study reflects the inherent complexity of ECL systems.[47,48,51,74−77] Apart from Φ_R, the ECL intensity may also be influenced by the oxidation potential of the complex (insofar as it dictates the thermodynamics of reaction 4 above), or by side reactions competing with reaction 1 or 4. Since the oxidizing power of the complexes is approximately constant, the most likely explanation for the observed trend is different susceptibilities to parasitic side reactions between the bipyridine- and phenanthroline-based complexes. This is in agreement with published work that showed that phenanthroline-based ruthenium complexes were relatively unstable in the oxidized form compared with $[Ru(bpy)_3]^{3+}$ [78] and is borne out (to an extent) in the i_p^{ox}/i_p^{red} data presented in Table 3.

dx.doi.org/10.1021/ic201911f | Inorg. Chem. 2011, 50, 12172−12183

CONCLUSION

The synthesis of four new Ru(II)-containing PNA-like monomers, $[Ru(bpy)_2(dpq\text{-}L\text{-}PNA{-}OH)]^{2+}$ (**M1**), $[Ru(phen)_2(dpq\text{-}L\text{-}PNA{-}OH)]^{2+}$ (**M2**), $[Ru(bpy)_2(dppz\text{-}L\text{-}PNA{-}OH)]^{2+}$ (**M3**), and $[Ru(phen)_2(dppz\text{-}L\text{-}PNA{-}OH)]^{2+}$ (**M4**) has been achieved. This new approach for preparing such Ru(II)−PNA monomers overcomes significant difficulties encountered in previously described syntheses. In addition, the key synthons, dpq-L-PNA and dppz-L-PNA, prepared en route can either be used directly for preparing other transition metal-PNA monomers for their subsequent incorporation at any chosen position within the PNA oligomer sequence or be employed for designing PNA templates to study metal coordination effects on the stability of such inorganic−nucleic acid duplexes, for nanotechnology applications. The UV/vis absorbance and emission spectra showed profiles characteristic of Ru(II) polypyridyl complexes, viz., a MLCT band centered around 450 nm and distinctive emission maxima (610−660 nm). Electrochemical studies on **M1**−**M4** showed them to undergo a reversible one-electron Ru^{II}/Ru^{III} oxidation process at a positive potential of *ca.* 950 mV (vs $Fc^{0/+}$). The measurements showed the Ru(II)−PNA monomers to be ECL-active luminophores. All of the monomers exhibited reasonably intense ECL emission in the presence of a TPA coreactant, with the bipyridine-based complexes **M1** and **M3** showing the highest ECL intensity. The data highlight the fact that compounds having the highest photoluminescence efficiency will not necessarily produce the most intense ECL because other, non-photophysical parameters may come into play. Overall, the photoluminescence and redox properties as well as the efficient ECL signal obtained from the prepared Ru(II)−PNA monomers identifies their scope and utility in designing multimodal Ru(II)−PNA oligomeric labels for biosensing applications.

ASSOCIATED CONTENT

Supporting Information

^1H NMR spectra of **M1**−**M4** (Figures S1−S4) and cyclic voltammograms of **M1**−**M4** as a function of scan rate (Figures S5−S8). This material is available free of charge via the Internet at http://pubs.acs.org.

AUTHOR INFORMATION

Corresponding Author

*Fax: +61 3 9905 4597. E-mail: Leone.Spiccia@monash.edu.

ACKNOWLEDGMENTS

This work was supported by the Australian Research Council through the Australian Centre of Excellence for Electromaterials Science (L.S.). T.J. is a recipient of Monash Graduate Scholarship and Monash International Postgraduate Research Scholarship. PSF acknowledges funding from the Australian Research Council (Future Fellowship) and Deakin University.

REFERENCES

(1) Nielsen, P. E.; Egholm, M.; Berg, R. H.; Buchardt, O. *Science* **1991**, *254*, 1497.
(2) Egholm, M.; Buchardt, O.; Christensen, L.; Behrens, C.; Freier, S. M.; Driver, D. A.; Berg, R. H.; Kim, S. K.; Norden, B.; Nielsen, P. E. *Nature* **1993**, *365*, 566.
(3) Egholm, M.; Buchardt, O.; Nielsen, P. E.; Berg, R. H. *J. Am. Chem. Soc.* **1992**, *114*, 1895.
(4) Hyrup, B.; Nielsen, P. E. *Bioorg. Med. Chem.* **1996**, *4*, 5.
(5) Good, L.; Nielsen, P. E. *Antisense Nucleic Acid Drug Dev.* **1997**, *7*, 431.
(6) Eldrup, A. B.; Nielsen, P. E. *Adv. Amino Acid Mimetics Peptidomimetics* **1999**, *2*, 221.
(7) Nielsen, P. E. *Pharmacol. Toxicol.* **2000**, *86*, 3.
(8) Nielsen, P. E. *Curr. Opin. Biotechnol.* **2001**, *12*, 16.
(9) Nielsen, P. E. *Lett. Pept. Sci.* **2004**, *10*, 135.
(10) Nielsen, P. E. *Chem. Biodivers.* **2007**, *4*, 1996.
(11) Egholm, M.; Nielsen, P. E.; Buchardt, O.; Berg, R. H. *J. Am. Chem. Soc.* **1992**, *114*, 9677.
(12) Ratilainen, T.; Holmen, A.; Tuite, E.; Haaima, G.; Christensen, L.; Nielsen, P. E.; Norden, B. *Biochemistry* **1998**, *37*, 12331.
(13) Buchardt, O.; Egholm, M.; Berg, R. H.; Nielsen, P. E. *Trends Biotechnol.* **1993**, *11*, 384.
(14) Nielsen, P. *Curr. Opin. Biotechnol.* **1999**, *10*, 71.
(15) Nielsen, P. E. *Acc. Chem. Res.* **1999**, *32*, 624.
(16) Gasser, G.; Sosniak, A. M.; Metzler-Nolte, N. *Dalton Trans.* **2011**, *40*, 7061.
(17) Verheijen, J. C.; van der Marel, G. A.; van Boom, J. H.; Metzler-Nolte, N. *Bioconjugate Chem.* **2000**, *11*, 741.
(18) Hess, A.; Metzler-Nolte, N. *Chem. Commun.* **1999**, 885.
(19) Baldoli, C.; Cerea, P.; Giannini, C.; Licandro, E.; Rigamonti, C.; Maiorana, S. *Synlett* **2005**, *13*, 1984.
(20) Ma, Z.; Olechnowicz, F.; Skorik, Y. A.; Achim, C. *Inorg. Chem.* **2011**, *50*, 6083.
(21) Franzini, R. M.; Watson, R. M.; Patra, G. K.; Breece, R. M.; Tierney, D. L.; Hendrich, M. P.; Achim, C. *Inorg. Chem.* **2006**, *45*, 9798.
(22) Wang, J. *Biosens. Bioelectron.* **1998**, *13*, 757.
(23) Li, C.; Li, X.; Liu, X.; Kraatz, H.-B. *Anal. Chem.* **2010**, *82*, 1166.
(24) Mokhir, A.; Stiebing, R.; Kraemer, R. *Bioorg. Med. Chem. Lett.* **2003**, *13*, 1399.
(25) Zelder, F. H.; Mokhir, A. A.; Krämer, R. *Inorg. Chem.* **2003**, *42*, 8618.
(26) Hamzavi, R.; Happ, T.; Weitershaus, K.; Metzler-Nolte, N. *J. Organomet. Chem.* **2004**, *689*, 4745.
(27) Mokhir, A.; Krämer, R.; Wolf, H. *J. Am. Chem. Soc.* **2004**, *126*, 6208.
(28) Gasser, G.; Belousoff, M. J.; Bond, A. M.; Spiccia, L. *J. Org. Chem.* **2006**, *71*, 7565.
(29) Xavier, C.; Giannini, C.; Dall'Angelo, S.; Gano, L.; Maiorana, S.; Alberto, R.; Santos, I. *J. Biol. Inorg. Chem.* **2008**, *13*, 1345.
(30) Gasser, G.; Brosch, O.; Ewers, A.; Weyhermuller, T.; Metzler-Nolte, N. *Dalton Trans.* **2009**, 4310.
(31) Gasser, G.; Neukamm, M. A.; Ewers, A.; Brosch, O.; Weyhermüller, T.; Metzler-Nolte, N. *Inorg. Chem.* **2009**, *48*, 3157.
(32) Gasser, G.; Husken, N.; Koster, S. D.; Metzler-Nolte, N. *Chem. Commun.* **2008**, 3675.
(33) Ferri, E.; Donghi, D.; Panigati, M.; Prencipe, G.; D'Alfonso, L.; Zanoni, I.; Baldoli, C.; Maiorana, S.; D'Alfonso, G.; Licandro, E. *Chem. Commun.* **2010**, *46*, 6255.
(34) Gasser, G.; Sosniak, A. M.; Leonidova, A.; Braband, H.; Metzler-Nolte, N. *Aust. J. Chem.* **2011**, *64*, 265.
(35) Baldoli, C.; Maiorana, S.; Licandro, E.; Zinzalla, G.; Perdicchia, D. *Org. Lett.* **2002**, *4*, 4341.
(36) Gasser, G.; Spiccia, L. *J. Organomet. Chem.* **2008**, *693*, 2478.
(37) Nickita, N.; Gasser, G.; Bond, A. M.; Spiccia, L. *Eur. J. Inorg. Chem.* **2009**, 2179.
(38) Hüsken, N.; Gasser, G.; Köster, S. D.; Metzler-Nolte, N. *Bioconjugate Chem.* **2009**, *20*, 1578.
(39) Hüsken, N.; Gębala, M.; Schuhmann, W.; Metzler-Nolte, N. *ChemBioChem* **2010**, *11*, 1754.
(40) van Staveren, D. R.; Metzler-Nolte, N. *Chem. Rev.* **2004**, *104*, 5931.
(41) Tucker, J. H. R.; Collinson, S. R. *Chem. Soc. Rev.* **2002**, *31*, 147.
(42) Juris, A.; Balzani, V.; Barigelletti, F.; Campagna, S.; Belser, P.; von Zelewsky, A. *Coord. Chem. Rev.* **1988**, *84*, 85.
(43) Spiccia, L.; Deacon, G. B.; Kepert, C. M. *Coord. Chem. Rev.* **2004**, *248*, 1329.

(44) Medlycott, E. A.; Hanan, G. S. *Chem. Soc. Rev.* **2005**, 34.
(45) Vos, J. G.; Kelly, J. M. *Dalton Trans.* **2006**, 4869.
(46) Fernández-Moreira, V.; Thorp-Greenwood, F. L.; Coogan, M. P. *Chem. Commun.* **2010**, *46*, 186.
(47) Barbante, G. J.; Hogan, C. F.; Wilson, D. J. D.; Lewcenko, N. A.; Pfeffer, F. M.; Barnett, N. W.; Francis, P. S. *Analyst* **2011**, *136*, 1329.
(48) Zhou, M.; Robertson, G. P.; Roovers, J. *Inorg. Chem.* **2005**, *44*, 8317.
(49) Kiran, R. V.; Zammit, E. M.; Hogan, C. F.; James, B. D.; Barnett, N. W.; Francis, P. S. *Analyst* **2009**, *134*, 1297.
(50) Tokel-Takvoryan, N.; Hemingway, R.; Bard, A. J. *J. Am. Chem. Soc.* **1973**, *95*, 6582.
(51) Bard, A. J. *Electrogenerated Chemiluminescence*; Marcel Dekker: New York, 2004.
(52) Richter, M. *Chem. Rev.* **2004**, *104*, 3003.
(53) Gorman, B.; Francis, P.; Barnett, N. *Analyst* **2006**, *131*, 616.
(54) Pyati, R.; Richter, M. *Annu. Rep. Prog. Chem. Sect. C: Phys. Chem.* **2007**, *103*, 12.
(55) Marquette, C.; Blum, L. *Anal. Bioanal. Chem.* **2008**, *390*, 155.
(56) Miao, W. *Chem. Rev.* **2008**, *108*, 2506.
(57) Forster, R. J.; Bertoncello, P.; Keyes, T. E. *Annu. Rev. Anal. Chem.* **2009**, *2*, 359.
(58) Su, M.; Liu, S. *Anal. Biochem.* **2010**, *402*, 1.
(59) Zhao, Q.; Huang, C.; Li, F. *Chem. Soc. Rev.* **2011**, *40*, 2508.
(60) van der Tol, E. B.; van Ramesdonk, H. J.; Verhoeven, J. W.; Steemers, F. J.; Kerver, E. G.; Verboom, W.; Reinhoudt, D. N. *Chem.—Eur. J.* **1998**, *4*, 2315.
(61) Dutta, S.; Kim, S.-K.; Patel, D. B.; Kim, T.-J.; Chang, Y. *Polyhedron* **2007**, *26*, 3799.
(62) Che, G.; Li, W.; Kong, Z.; Su, Z.; Chu, B.; Li, B.; Zhang, Z.; Hu, Z.; Chi, H. *Synth. Commun.* **2006**, *36*, 2519.
(63) Thomson, S. A.; Josey, J. A.; Cadilla, R.; Gaul, M. D.; Fred Hassman, C.; Luzzio, M. J.; Pipe, A. J.; Reed, K. L.; Ricca, D. J.; Wiethe, R. W.; Noble, S. A. *Tetrahedron* **1995**, *51*, 6179.
(64) Sullivan, B. P.; Salmon, D. J.; Meyer, T. J. *Inorg. Chem.* **1978**, *17*, 3334.
(65) Kissinger, T.; Heineman, W. R. In *Laboratory Techniques in Electroanalytical Chemistry*, 2nd ed.; Marcel Dekker Inc.: New York: 1996, p 469.
(66) Gottlieb, H. E.; Kotlyar, V.; Nudelman, A. *J. Org. Chem.* **1997**, *62*, 7512.
(67) Nickita, N.; Gasser, G.; Pearson, P.; Belousoff, M. J.; Goh, L. Y.; Bond, A. M.; Deacon, G. B.; Spiccia, L. *Inorg. Chem.* **2008**, *48*, 68.
(68) Nickita.; Belousoff, M. J.; Bhatt, A. I.; Bond, A. M.; Deacon, G. B.; Gasser, G.; Spiccia, L. *Inorg. Chem.* **2007**, *46*, 8638.
(69) Lo, K. K.-W.; Lee, T. K.-M. *Inorg. Chim. Acta* **2007**, *360*, 293.
(70) Nicholson, R. S. *Anal. Chem.* **1966**, *38*, 1406.
(71) Bard, A. J.; Faulkner, L. R. *Electrochemical Methods, Fundamentals and Application*, 2nd ed.; Brisbane, Australia, 2001.
(72) Sevick, A. *Collect. Czech. Chem. Commun.* **1948**, *13*, 349.
(73) Randles, J. E. B. *Trans. Faraday Soc.* **1948**, *44*, 327.
(74) Leland, J. K.; Powell, M. J. *J. Electrochem. Soc.* **1990**, *137*, 3127.
(75) Miao, W.; Choi, J.; Bard, A. J. *J. Am. Chem. Soc.* **2002**, *124*, 14478.
(76) Wightman, R. M.; Forry, S. P.; Maus, R.; Badocco, D.; Pastore, P. *J. Phys. Chem. B* **2004**, *108*, 19119.
(77) Barbante, G. J.; Hogan, C. F.; Mechler, A.; Hughes, A. B. *J. Mater. Chem.* **2010**, *20*, 891.
(78) Cooke, M. M.; Doeven, E. H.; Hogan, C. F.; Adcock, J. L.; McDermott, G. P.; Conlan, X. A.; Barnett, N. W.; Pfeffer, F. M.; Francis, P. S. *Anal. Chim. Acta* **2009**, *635*, 94.